Jurnal Kejuruteraan 38(4) 2026: 1785-1796
https://doi.org/10.17576/jkukm-2026-38(4)-19

TR-Net: Deep Learning Based Transformer Monitoring

Marizuana Mat Daud[a*], Nur Badariah Ahmad Mustafa[b], Swee Xiao Qi[b] & Hidayat Zainuddin[c]

[a]*Institute of Visual Informatics, Technopolis Cyber Academia, Universiti Kebangsaan Malaysia, 43600 Bangi, Malaysia*

[b]*Institute of Power Engineering, Department of Electrical and Electronics Engineering, College of Engineering, Universiti Tenaga Nasional, 43000 Kajang, Malaysia*

[c]*Faculty of Electrical Engineering, Universiti Teknikal Malaysia, 76100 Durian Tunggal, Malaysia*

[*]*Corresponding author: marizuana.daud@ukm.edu.my*

Received 21 March 2025, Received in revised form 4 January 2026
Accepted 4 February 2026, Available online 30 July 2026

ABSTRACT

Transformer oil is a vital insulating medium for maintaining the dielectric strength of power transformers due to its thermal stability and electrical insulating properties. However, conventional gas-based monitoring techniques often fail to detect early cellulose bridging, which can result in insulation failure and transformer breakdown if not addressed through timely maintenance. To overcome this limitation, this study proposes a deep learning (DL)–based approach for predicting transformer oil health condition. Transformer oil condition is assessed by analysing images captured from laboratory experiments that simulate cellulose bridging formation. The visual patterns are categorised into three stages: pre-bridging, bridging, and post-bridging, where pre-bridging and bridging represent pre-breakdown conditions, and post-bridging indicates the after-breakdown state. Image classification is performed using a pretrained AlexNet model and a modified version, TR-Net. A dataset of 1,800 cellulose bridging images, equally distributed across the three classes, is used for training and evaluation. The dataset includes both original and augmented images to improve robustness. The models are trained using optimised hyperparameters, including Stochastic Gradient Descent with Momentum (SGDM), with carefully selected epoch numbers, batch sizes, learning rates, and convolutional layer configurations. Results show that TR-Net achieves a higher confidence level of 0.97 with a shorter training time of 72 minutes and 50 seconds, compared to the pretrained AlexNet, which attains a confidence level of 0.90 with a training time of 86 minutes and 45 seconds. These findings demonstrate that TR-Net provides improved accuracy and efficiency for automated transformer oil condition assessment without human intervention.

Keywords: Deep learning; cellulose bridging; image classification; transformer breakdown; transformer oil

INTRODUCTION

The rapid expansion of High Voltage Direct Current (HVDC) power transmission systems has driven significant improvements in power distribution network efficiency. HVDC transformers are critical components in these electrical power systems, serving as coupling elements between high-power rectifiers and AC grids. They facilitate the transmission of electrical power from grids to end users with minimal loss. Transformer oil plays a vital role in maintaining the efficiency of these transformers. It serves two primary functions: as an insulating medium to maintain the transformer's dielectric strength, and as a coolant to dissipate heat. This dielectric liquid exhibits stability at high temperatures and possesses outstanding electrical insulating properties (Leong et al. 2018).

However, transformer failures due to degraded insulating oil performance account for nearly 33% of all transformer malfunctions (Pan et al. 2018). Contamination of the transformer oil is a leading cause of insulation failure. This contamination can occur during packaging, transportation, or storage processes. In aged transformers, metallic particles and cellulosic fiber residuals are commonly found contaminants (Mustafa et al. 2020). During normal transformer operation, the insulating oil interacts with various internal components such as metals, iron cores, windings, and insulation papers. This interaction, combined with electrical and thermal stresses, contributes to the presence of contaminants in the oil (Zainoddin et al. 2017). Understanding and mitigating these contamination issues is crucial for maintaining the reliability and efficiency of HVDC power transmission systems. Effective monitoring and maintenance of transformer oil quality can significantly reduce the risk of transformer failure and improve the overall performance of power distribution networks.

RELATED WORKS

Many transformer monitoring techniques have been introduced that includes the internal and external transformer failures. Internal failures occur within the transformer itself. The techniques proposed by previous researchers to detect the internal failures were thermal analysis, vibrational analysis, movement of winding, dissolved gas analysis (DGA) and partial discharge (PD) analysis (Chandran et al. 2021), (Kherif et al. 2021). The offline DGA monitoring technique has been adopted long time ago, however, the technique is less reliable, required a long period for gases restoring process. For a real-time monitoring, thermal imaging has been proposed to analyze the thermal map of the transformer structure. It is an effective non-destructive testing that can be performed during maintenance (Chandran et al. 2021). Despite that, the thermal images obtained from the testing is not feasible to integrate with various control techniques and the monitoring status is also dependent to image classifying algorithms. Rupali Balabantaraya et. al. (Balabantaraya et al. 2024) proposed the deep learning techniques such as modified VGG-16 to evaluate thermal images and identify the transformer status as good or defect. The monitoring of transformer health status is based on the remarkable temperature rise seen on thermal images. The modified VGG-16 achieved an accuracy of 99% and effectively handled large datasets of complex thermal images of the transformer. However, the study lacks in evaluation of the transformer condition under varying loads and different environmental conditions.

For the past five years, various machine learning (ML) techniques have been explored to assess transformer oil condition (Kherif et al. 2021) (Rediansyah et al. 2021). The use of artificial intelligence (AI) techniques to enhance DGA diagnostics has been on the rise. Omar Kherif et. al. conducted a study on improving the diagnostic accuracy of DGA for power transformer faults by combining K-Nearest Neighbors (KNN) classifier with decision tree (DT) principles. This study utilized five hydrocarbon gases (H2, CH4, C2H2, C2H4, and C2H6), achieving a global accuracy rate exceeding 93% for diagnosing power transformer faults. Taha and Mansour (Taha and Mansour, 2021) introduced power transformer fault diagnostic using optimized machine learning techniques. The research team developed sophisticated diagnostic tools leveraging DGA data, specifically focusing on four key gases: hydrogen (H2), methane (CH4), ethane (C2H6), and acetylene (C2H2). To enhance the accuracy and reliability of fault detection, the study employed data transformation techniques in conjunction with six optimized machine learning (OML) methods; Decision Trees (DT), Discriminant Analysis (DA), Naïve Bayes (NB), Support Vector Machines (SVM), K-Nearest Neighbors (KNN) and Ensemble Methods (EN). Prior to applying these OML classification techniques, the researchers implemented data transformation strategies. This crucial preprocessing step was designed to mitigate the significant overlap observed in the distribution of different gases across various fault types within the dataset. By reducing this overlap, the team aimed to enhance the discriminative power of the subsequent machine learning models, potentially leading to more accurate and reliable fault diagnoses in transformer systems.

This comprehensive approach, combining advanced data preprocessing with a diverse array of machine learning techniques, represents a significant step forward in the development of robust and efficient diagnostic tools for transformer fault detection and classification. This proposed approach demonstrated that combining gas percentage transformation with the EN achieve higher accuracy of 90.61% compared to other OML methods.

Research on determining the health index (HI) of transformer condition, based on oil quality, DGA, and insulation paper condition, compared seven ML algorithms (Rediansyah et al. 2021). In this study, the random forest (RF) algorithm emerged as the most effective, achieving 97.3% accuracy in measuring the transformer condition HI. These findings underscore the potential of ML techniques in enhancing transformer oil condition assessment and fault diagnosis in power systems.

The AlexNet model, a convolutional neural network (CNN) architecture, has played a pivotal role in advancing computer vision and deep learning. Recognized as a pioneering model, AlexNet popularized the use of deep neural networks for image classification tasks. AlexNet is a productive deep learning model utilized for understanding image contents and creating state-of-the-art functions in image recognition, segmentation, and detection (Khumaidi et al. 2017). Image classification using AlexNet offers the advantage of automatic feature extraction through convolutional layers, eliminating the need for manual feature extraction (Chen et al. 2019). The AlexNet architecture comprises eight critical layers: one input layer, two convolutional layers, two pooling layers, two fully connected layers, and one output layer. This model has been adopted and improvised in various studies, particularly for fault detection in high voltage electrical equipment and conventional circuit breakers (Ullah et al. 2020) (Sun et al. 2020). Figure 1 illustrates the basic AlexNet architecture.

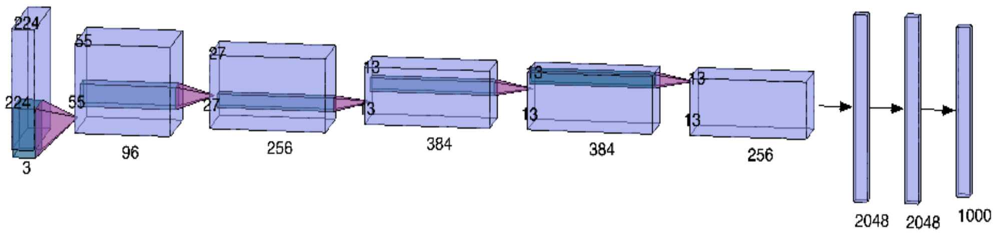

FIGURE 1. Basic AlexNet architecture

In (Ullah et al. 2020), a pretrained AlexNet model was employed to extract features from captured infrared images of high voltage equipment. These extracted features were then used to train Random Forest (RF) and SVM classifiers to identify defective and non-defective high voltage equipment, with RF achieving 96% accuracy. Another investigation improved the AlexNet model for fault diagnosis in the contact system of conventional circuit breakers. This enhanced method achieved an accuracy of 99.46% using time-frequency images and 97.45% using 1-D series signals (Sun et al. 2020). These applications demonstrate the versatility and effectiveness of the AlexNet model in addressing complex image classification tasks in electrical engineering contexts.

However, based on our current knowledge, there is a limited amount of literature available for recognizing the transformer oil condition, specifically in terms of the oil's dielectric strength, based on captured images of cellulose bridging formations. The main contributions of this research are summarised as follows:

1. Image-Based Assessment of Transformer Oil Condition

   This research introduces a direct image-based approach for assessing transformer oil condition by analysing cellulose bridging formations, addressing the lack of existing studies that focus on visual indicators of dielectric degradation during pre-breakdown stages.

2. Classification of Pre-Breakdown and Breakdown Stages

   The study formulates the transformer oil condition assessment problem as a multi-class classification task, categorising visual patterns into pre-bridging, bridging, and post-bridging stages, where pre-bridging and bridging correspond to pre-breakdown conditions.

3. Development of a Deep Learning–Based Monitoring Framework (TR-Net)

   A novel deep learning model, referred to as TR-Net, is developed to automatically detect and classify cellulose bridging stages without human intervention, enabling early identification of insulation degradation.

4. Alternative to Conventional Gas-Based Diagnostic Methods

   The proposed visual monitoring approach provides a complementary alternative to traditional gas and thermal analysis methods, which often fail to detect early-stage degradation and are susceptible to external operating conditions.

5. Support for Early Maintenance Decision-Making

   By enabling early and reliable detection of pre-breakdown conditions, the proposed method supports timely maintenance decisions and contributes to improved transformer reliability and failure prevention.

The paper is organized as follows: the first section provides a brief introduction to the conventional and current methods for diagnosing transformers. The second section discusses TR-Net's approach and how the experiment was executed. The next part covers the findings and discussion of transformer monitoring with TR-Net. The final section presents the research's conclusion and future work.

METHODOLOGY

The methodology consists of five-step process (shown in Figure 2): (a) dataset preparation, (b) data augmentation, (c) pretrained model, (d) TR-Net model and (e) evaluation. The process begins with dataset preparation, where the data is split into training, testing, and validation sets. Next, data augmentation is performed to artificially increase the size of the dataset, potentially improving model robustness. The third step involves training using a pretrained model, leveraging transfer learning to potentially improve performance and reduce training time. Following this, a TR-Net model is trained, which a modified AlexNet architecture designed for the task at hand. Finally, the process concludes with an evaluation step, where metric evaluation is performed on the validation dataset to assess the model's performance. This systematic approach ensures a thorough development cycle from data preparation to final model assessment.

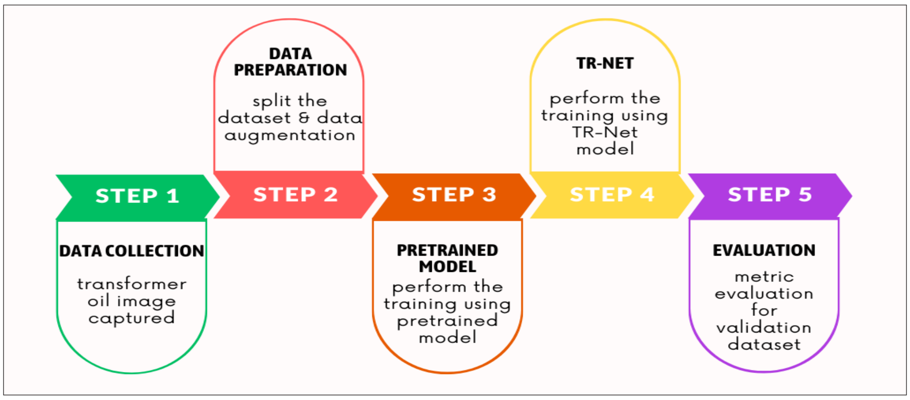

FIGURE 2. Flow diagram of the proposed method

DATA COLLECTION

This study begins with the gathering of cellulose bridging formation images for pre-bridging, bridging, and post-bridging classes from three transformer oil samples: Gemini X, MIDEL 7131, and PFAE [3]. The cellulose bridging image samples were obtained during laboratory setting studies. In the cellulose bridging studies, one electrode received a high voltage direct current (HVDC), while the other was grounded. The supply voltage was gradually increased in stages of one minute at each voltage level (2kV, 7kV, and 10kV) until it reached 5kV, right before breakdown. The goal of increasing the voltage level was to explore the DEP phenomena, specifically particle mobility, beginning with a static condition and advancing to a full (thicker) bridge between the electrodes. The time intervals between voltage steps were generally between three and five seconds. Figure 3 shows the laboratory setup for the cellulose bridging experiment. The collected image samples served as input data images, which were shown in the red, green, and blue (RGB) color scheme.

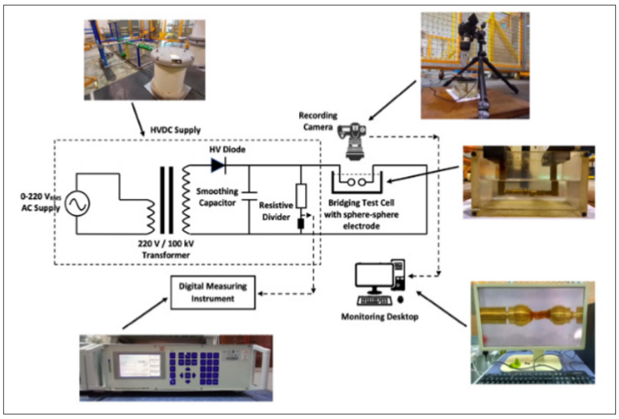

FIGURE 3. Laboratory setup for cellulose particles bridging experiments

Table 1 displays the RGB images representing pre-bridging, bridging, and post-bridging classes obtained from the cellulose bridging experiment. In pre-bridging stage, the oil or cellulose starts forming a connection between the two metal surfaces. This is visually represented by the material stretching across the gap, creating a bridge. It appears more compact in the center, and some particles may accumulate in the middle, indicating that the bridging process is underway. However, the bridge is not yet fully stable or continuous. For bridging phase, a full and stable bridge is clearly visible between the two metal surfaces.

TABLE 1. The samples of RGB image of pre-bridging, bridging and post-bridging classes

Image class	RGB image
Pre-bridging	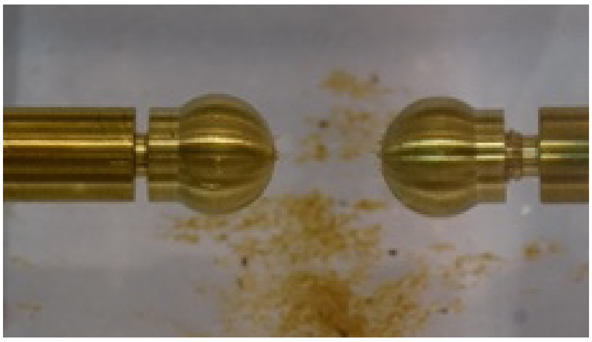
Bridging	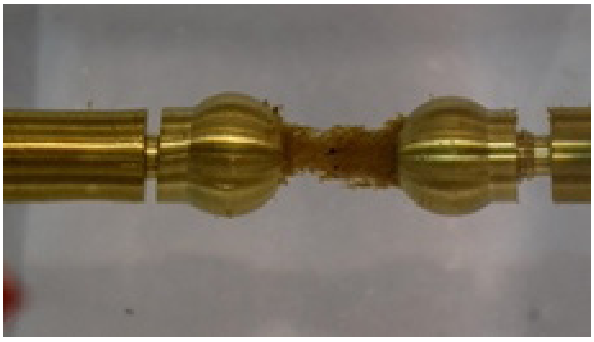
Post-bridging	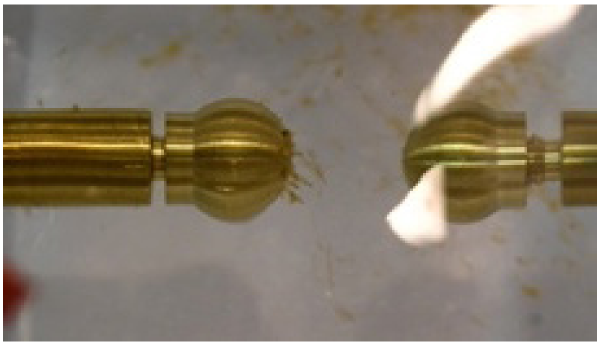

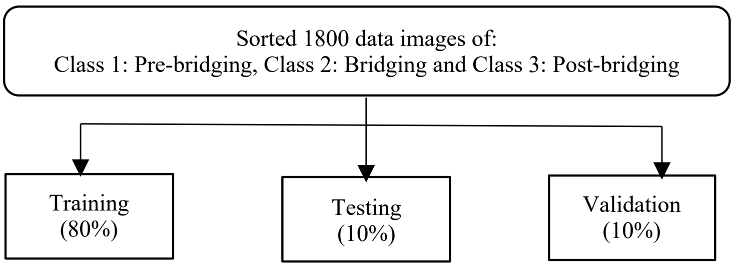

FIGURE 4. Dataset preparation with splitting portion of 80:10:10.

The oil or cellulose particles now form a continuous, thickened pathway connecting the two sides. This stage signifies that the bridging process has been completed, and the metal surfaces are linked through the bridge formed by the cellulose particles. Lastly, during the post-bridging stage, the cellulose particles dispersed and fell to the base of the experiment due to the explosion that occurred during the breakdown.

FIGURE 5. A complete process of training and testing using pretrained Alexnet model.

The MATLAB Image Batch Processor offers a streamlined approach to data augmentation. It generates an output folder containing the processed images while maintaining the original file names and subfolder structure of the input folder. This user-friendly application minimizes manual intervention, making the creation and organization of output folders for dataset tools, we were able to expand the training dataset systematically, introducing controlled variations that improve the model's robustness and performance across a wider range of input scenarios. This approach not only enhances the model's learning capacity but also contributes to its ability to handle real-world data variability more effectively. The methods chosen for this study were data resizing, rotation, translation and reflection. Table 2 depicts the samples of original and augmented images of pre-bridging, bridging and post-bridging classes.

After preparing the dataset, the training dataset were fed into AlexNet network for image classification process. For this study, two distinct AlexNet models namely pretrained and Modified AlexNet (TR-Net) models were designed and compared in terms of their accuracy performance. AlexNet model was chosen because its architecture has a least number of total layers and ratio of weight transfer (less complex), highest accuracy and least training time (Khagi and Kwon, 2019). Following sections described the detailed architectures of both the pretrained and modified AlexNet models.

PRETRAINED ALEX NET

As shown in Fig 5, the flow diagram of the complete process, start with pretrained model loaded, then final layers replaced with new layers and learn of new features. Next, train the network using input training images with some hyperparameter setup. Finally, a prediction performed using test images. The study utilized a pretrained AlexNet model, comprising 25 layers, which was imported from the MATLAB library using the function *net*=alexnet (MathWorks, 2024). This sophisticated neural network architecture features a single input layer designed to process images with dimensions of 227-by-227-by-3 pixels.

The model's core consists of five convolutional layers, each employing different filter sizes, padding, and stride configurations to autonomously extract salient image features. To introduce non-linearity and enhance the model's ability to learn complex patterns, seven Rectified Linear Unit (ReLU) activation layers were integrated (Description, 2024). To standardize the scale of extracted features, two cross-normalization layers were incorporated (Trimakno and Kusrini, 2021). The network's ability to manage spatial hierarchies was further augmented by three max pooling layers, which create down-sampled feature maps (Image and Random, n.d.). For high-level reasoning, the architecture includes three fully connected layers. These layers perform matrix multiplication on the input, followed by the addition of a bias vector, enabling the network to make intricate associations between features (MathWorks, 2024).

The final fully connected layer of the pretrained AlexNet is composed of 1000 neurons, each corresponding to a distinct class from the original training dataset. This configuration allows the network to classify inputs into a wide array of categories, demonstrating its versatility and potential for transfer learning in various domains. In this study, the number of neurons were reduced to three neurons to suit the outcome of the network that were pre-bridging, bridging and post-bridging classes. The dropout layers were used to avoid overfitting [22]. Finally, the output layer was placed at the end of pretrained AlexNet model for image classification.

TR-NET

The study employed a modified AlexNet architecture, designated as TR-Net, comprising 28 layers for training the dataset. This adaptation aimed to enhance network performance by reducing loss, optimizing training time, and increasing classification confidence levels. The TR-Net architecture begins with an input layer accepting 227x227x3 images, followed by five convolutional layers with varied filter sizes, padding, and stride configurations for automated feature extraction. Eight ReLU activation functions were integrated to transform nodal inputs into outputs. Two cross-normalization layers were incorporated to standardize feature scales, while three max pooling layers were implemented for feature map down sampling. The network includes four fully connected layers for weighted input multiplication and bias addition, three dropout layers to mitigate overfitting, and a final output layer for image classification. TR-Net architecture was built and trained using the Deep Network Designer. The trained model was then included into the algorithm for further image classification tasks, using the hyperparameter configuration detailed in Table 3.

TABLE 3. Hyperparameter tuning set up.

Types of hyperparameter	Value
Optimizer	SGDM
Epochs	20
Initial learning rate	0.001
Iteration	300

RESULT AND DISCUSSION

This section presents the performance evaluation of pretrained AlexNet and TR-Net. Both models were trained using the hyperparameters outlined in Table 3. The training process for the pretrained AlexNet, illustrated in Figure 6(a), required a total of 86 minutes and 45 seconds. The training accuracy curve for pretrained AlexNet began at 40% in the first epoch, followed by a rapid increase to 90% in the second epoch. Subsequently, the accuracy stabilized, indicating the optimal point to cease training to prevent overfitting. Notably, the pretrained AlexNet achieved a perfect 100% training accuracy. Given that the network structure of the pretrained AlexNet model was imported from MATLAB, the high likelihood of achieving perfect training accuracy was anticipated. Furthermore, the training curve maintained a consistent level of 99% without experiencing any significant drops or decreases, demonstrating the absence of overfitting in the pretrained AlexNet model.

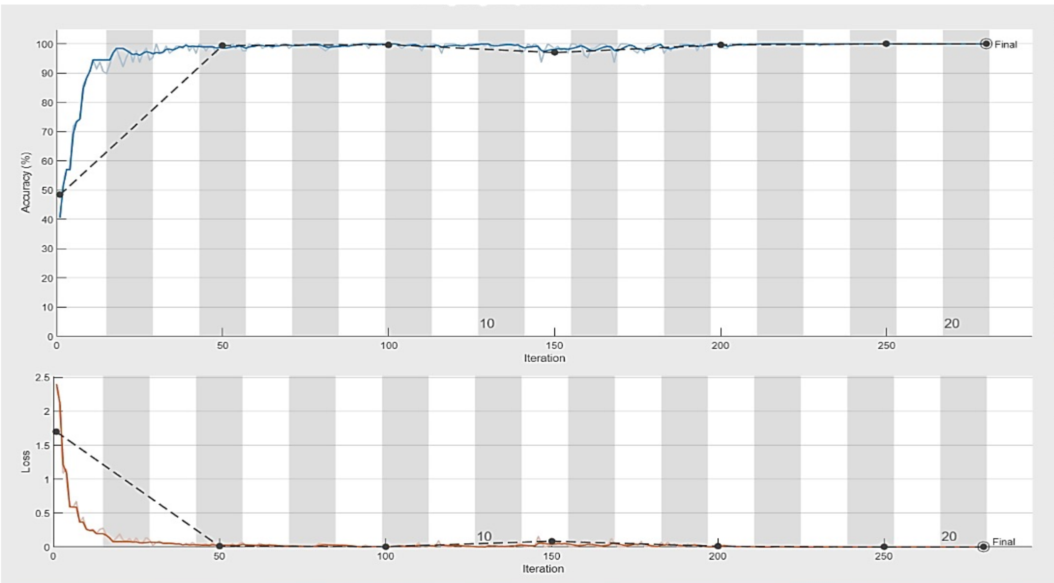

(a)

continue...

...cont.

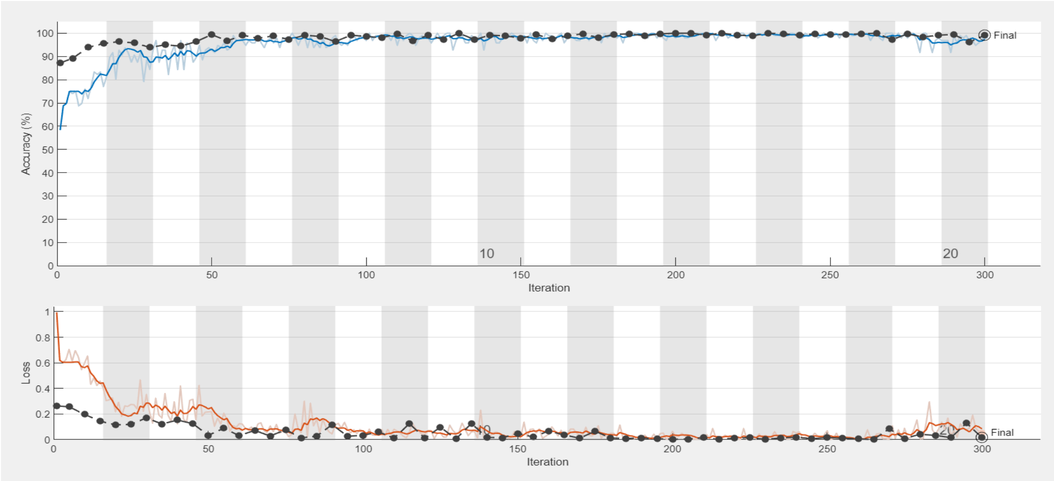

(b)

FIGURE 6. (a) Training progress of accuracy and loss graph for Pretrained AlexNet, (b) Training progress of accuracy and loss graph for TR-Net

To mitigate potential overfitting in training models, larger training datasets are recommended. In this study, 1,440 training images were utilized to train the 25 layers of the pretrained AlexNet model, which facilitated the achievement of 100% training accuracy. The training loss curve for pretrained AlexNet initiated with a value of 2.5 in the first epoch, rapidly decreasing to 0.25 in the second epoch. Subsequently, it stabilized at a minimum level. The pretrained AlexNet achieved a near-zero training loss, which is consistent with the perfect training accuracy and can be attributed to the network structure sourced from MATLAB. These results underscore the effectiveness of the pretrained AlexNet model in achieving high accuracy and low loss during the training process. However, it is important to note that while perfect training accuracy is impressive, it is crucial to evaluate the model's performance on a separate validation or test set to ensure its generalizability to unseen data.

The hyperparameter configuration for TR-Net closely mirrored that of the pretrained AlexNet, with the key distinction being its implementation within the deep network designer application. As illustrated in Figure 6 (b), TR-Net's training process concluded in 72 minutes and 50 seconds. TR-Net's training accuracy trajectory initiated at 60% in the first epoch, swiftly escalating to 75% in the second. It subsequently peaked at 92% before slightly regressing to 90%. The accuracy then stabilized, indicating the optimal juncture to terminate training to prevent overfitting. Ultimately, TR-Net achieved an impressive 99.17% training accuracy.

To mitigate overfitting risks, a dataset of 1,440 training images was employed to train TR-Net's 28 network layers. This robust dataset facilitated the network's ability to attain near-perfect training accuracy. The training loss curve for TR-Net commenced at 1.0 in the initial epoch, rapidly descending to 0.6 in the second, followed by a sharp decline to 0.2. Two minor fluctuations to 0.25 were observed (iteration<50) before the loss stabilized at a minimal level. By the final epoch, TR-Net exhibited near-zero training loss.

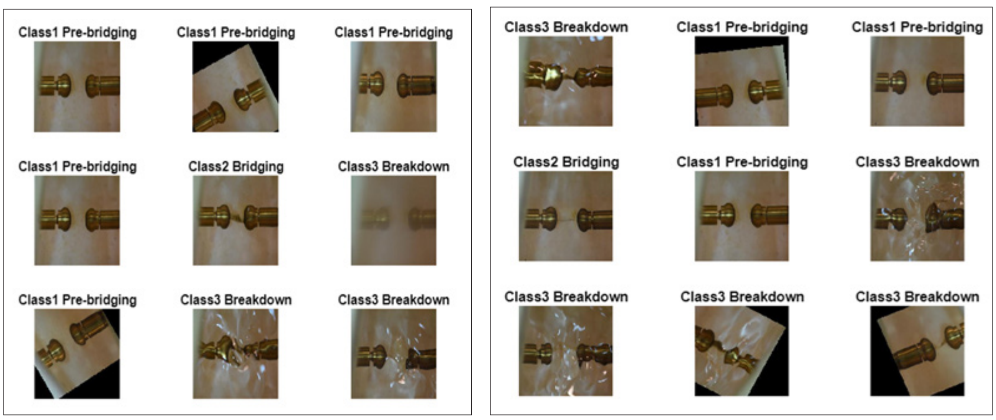

(a) (b)

FIGURE 7. Sample of evaluated testing images

Both pretrained AlexNet and TR-Net models demonstrated exceptional training performance, characterized by high accuracy and low loss. The marginal discrepancy in validation accuracy between TR-Net (99.17%) and pretrained AlexNet (100%) could be attributed to data variations or random fluctuations. Nonetheless, both models exhibit strong predictive capabilities.

To assess the models' generalization performance, a test set comprising 180 images was randomly selected from the total pool of 1,800 images. Figure 7 presents a sample of the evaluated testing images for both pretrained AlexNet and TR-Net. This comprehensive evaluation underscores the efficacy of both models in image classification tasks. While the pretrained AlexNet achieved perfect training accuracy, TR-Net's performance is nearly equivalent, suggesting that both models have effectively learned the underlying patterns in the training data. However, it is crucial to emphasize that the true measure of a model's effectiveness lies in its performance on unseen data, which is reflected in the test set results. The slight variation in accuracy between the two models on the validation set underscores the importance of rigorous testing to ensure robust and generalizable performance across diverse datasets.

The classification using the pretrained AlexNet and TR-Net models achieved 100% correct labeling for all classes (pre-bridging, bridging, and post-bridging). The finding was described in confusion matrix, which demonstrated a perfect match between the output and target classes across all three classes. Figure 8 depicted the confusion matrix illustrating the classification findings of both models. The confusion matrix provides a systematic representation of the prediction outcomes accuracy in relation to the original classes.

To assess the performance of the pretrained AlexNet and TR-Net models, a validation stage was conducted using images that were not part of the training process. The trained image samples were obtained from images captured with a 15mm electrode gap. However, in this work, images with 10mm and 20mm electrode gaps were considered, to measure the robustness of the models, as shown Figure 9.

Next, the validation process was extended to images captured by real-time webcam and hand-drawn images, as shown in Figure 10. The findings shown that the real-time webcam images were correctly classified across all classes with the confidence level range between 0.9 and 0.99 for pretrained AlexNet, while 0.99 to 1 for TR-Net, as simplify in Table 4. These findings lead to a conclusion that both models were not overfitted. The models demonstrated precise classification of images across different classes, even when the input images were not part of the training dataset. Its successfully managed variations in terms of scaling, brightness, and layout. The robustness of the model was also validated using a simple hand-drawn images that consist of two electrodes and cellulose in between electrodes.

The outcomes from the pretrained AlexNet shows the correct classification results with slightly lower confidence level. The confidence level of hand-drawn images was lower compared to pre-downloaded images from mobile device (real-time webcam). This is because the hand-drawn images were not trained in the pretrained AlexNet model. The hand-drawn images yielded correct classification findings with confidence level of 0.97, 0.39 and 0.54 for the pre-bridging, bridging and post-bridging classes, respectively.

TABLE 4. Comparing the confidence level of pre-trained AlexNet model and TR-Net model using real-time webcam images versus hand-drawn images

	Real-time webcam images			Hand-drawn images		
Models	Pre-bridging	Bridging	Post-bridging	Pre-bridging	Bridging	Post-bridging
Pre-trained Alexnet	0.99	0.90	0.99	0.97	0.39	0.54
TR-Net	1.0	0.99	0.99	0.96	0.69	0.77

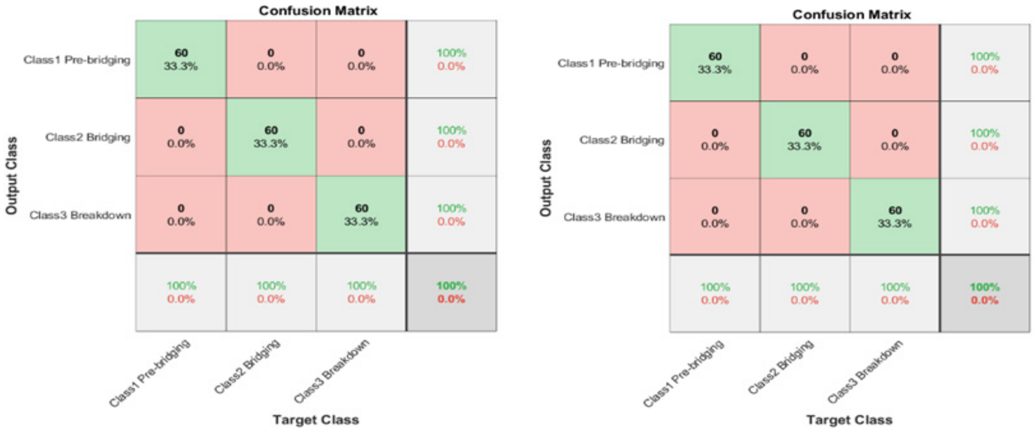

(a) Pretrained AlexNet (b) TR-Net

FIGURE 8. Confusion matrix for testing images

However, for TR-Net, the hand-drawn images yielded correct classification findings with confidence level of 0.96, 0.69 and 0.77 for the pre-bridging, bridging and post-bridging classes, respectively. These findings demonstrate the classification ability of TR-Net model on the newly added hand-drawn images and the pre-downloaded images from the webcam, as well as images captured with different electrodes gap.

CONCLUSION AND FUTURE WORKS

This study focused on the classification of cellulose particle bridging images using two models: a pretrained AlexNet and a proposed model, TR-Net. The architectural complexity of these models differs, with the pretrained AlexNet comprising 25 layers and the TR-Net featuring 28 layers. To assess the models' accuracy and confidence levels, they were evaluated using unseen data from validation and testing datasets. Remarkably, both models achieved 100% accuracy when tested on the designated testing dataset. To further validate their performance, the models were challenged with a variety of untrained images, including those with different electrode gaps (10mm and 20mm), real-time webcam captures, and hand-drawn images. Both models successfully classified all untrained images correctly.

However, a notable distinction emerged in the confidence levels for untrained images. The TR-Net consistently demonstrated higher confidence scores (pre-bridging: 0.96, bridging: 0.69, post-bridging: 0.77) compared to the pretrained AlexNet (pre-bridging: 0.97, bridging: 0.39, post-bridging: 0.54). This suggests that the proposed model TR-Net exhibits greater certainty in its classifications, particularly for bridging and post-bridging states. These findings underscore the effectiveness of both models in classifying cellulose particle bridging images, with the TR-Net showing particular promise in terms of training efficiency and classification confidence. The study highlights the potential for further optimization of deep learning models in this domain, potentially leading to more robust and efficient classification systems for particle bridging phenomena.

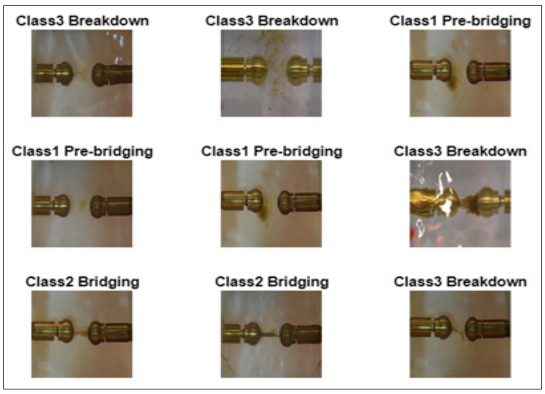

(a)Pretrained AlexNet

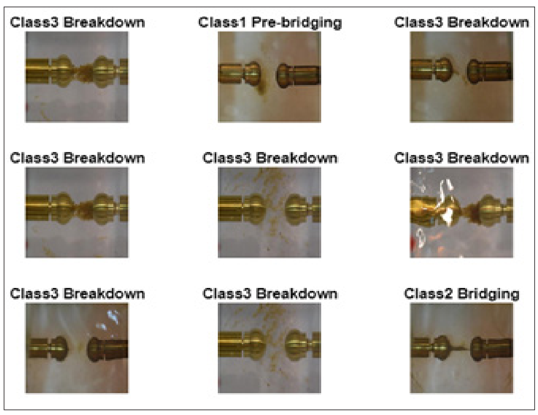

(b)TR-Net

FIGURE 9. Findings of untrained testing images of different electrodes gap (10mm and 20mm)

(a)Pretrained AlexNet

(b)TR-Net

FIGURE 10. Validation outcomes using real-time webcam and simple hand-drawn images (a) Pretrained AlexNet, (b) TR-Net.

For future works, a complete system and framework to be proposed to deploy TR-Net model in real-world application. For future works, a complete system and framework should be proposed to deploy the TR-Net model in real-world applications. This system needs to ensure scalability for handling large datasets and users, optimize inference speed to deliver real-time predictions, and be designed with cross-platform compatibility for seamless integration across multiple devices and platforms. These considerations will ensure the model's practical use in diverse environments while maintaining high performance.

ACKNOWLEDGEMENT

This work was carried out with the financial support from the Ministry of Higher Education under the Fundamental Research Grant Scheme (FRGS) number: FRGS/1/2020/TK0/UNITEN/02/17.

DECLARATION OF COMPETING INTEREST

None.

REFERENCES

Balabantaraya, R., Sahoo, A. K., Sahoo, P. K., Abir, C. M. & Panda, M. K. 2024. A novel infrared thermography image analysis for transformer condition monitoring. *Advances in Electrical Engineering, Electronics and Energy* 10: 100758.

Chen, E., Wu, X., Wang, C. & Du, Y. 2019. Application of improved convolutional neural network in image classification. In *Proceedings of the 2019 International Conference on Machine Learning, Big Data and Business Intelligence (MLBDBI)*, pp. 109-113.

Chandran, L. R., Babu, G. S. A., Nair, M. G. & Ilango, K. 2021. A review on status monitoring techniques of transformer and a case study on loss of life calculation of distribution transformers. *Materials Today: Proceedings* 46: [page range incomplete].

Description, P. 2024. Resize Port Description. *MathWorks Documentation*. Accessed 2 December 2024. https://www.mathworks.com/help/vision/ref/resize.html?searchHighlight=resize&s_tid=srchtitle_resize_1

Image, T. & Processor, B. 2024. Image Batch Processor. *MathWorks Documentation*. Accessed 2 December 2024. https://www.mathworks.com/help/images/batch-processing-using-the-image-batch-processorapp.html

Image, R. & Random, B. n.d. Open in MATLAB Online Copy Command. pp. 1-9.

Khagi, B. & Kwon, G. R. 2019. CNN model performance analysis on MRI images of an OASIS dataset for distinction between healthy and Alzheimer's patients. *IEIE Transactions on Smart Processing and Computing* 8(4): 272-278.

Kherif, O., Benmahamed, Y., Teguar, M., Boubakeur, A. & Ghoneim, S. S. 2021. Accuracy improvement of power transformer faults diagnostic using KNN classifier with decision tree principle. *IEEE Access* 9: 81693-81701.

Khumaidi, A., Yuniarno, E. M. & Purnomo, M. H. 2017. Welding defect classification based on convolution neural network (CNN) and Gaussian kernel. In *Proceedings of the 2017 International Seminar on Intelligent Technology and Its Applications (ISITIA)*, pp. 261-265.

Korzhebin, T. A. & Egorov, A. D. 2021. Comparison of combinations of data augmentation methods and transfer learning strategies in image classification used in convolution deep neural networks. In *Proceedings of the 2021 IEEE Conference of Russian Young Researchers in Electrical and Electronic Engineering (ElConRus)*, pp. 479-482. https://doi.org/10.1109/ElConRus51938.2021.9396724

Leong, Y. S. et al. 2018. UV-vis spectroscopy: A new approach for assessing the color index of transformer insulating oil. *Sensors* 18(7): 1-15.

MathWorks. 2024. AlexNet convolutional neural network. *MathWorks Documentation*. Accessed 2 December 2024. https://la.mathworks.com/help/deeplearning/ref/alexnet.html

Mustafa, N. B. A., Ali, N. H. N., Zainuddin, H., Daud, M. M. & Nordin, F. H. 2020. Electric field bridging pattern of pre-breakdown and breakdown condition in transformer oil. *Indonesian Journal of Electrical Engineering and Computer Science* 19(3): 1210-1218.

Pan, C., Tang, J., Tao, X., Zhang, Y. & Ma, S. 2018. Partial discharge and breakdown characteristics of moving transformer oil contaminated by metallic particles. *IEEE Transactions on Dielectrics and Electrical Insulation* 25(5): 1774-1784.

Policy, C., Settings, C. & Cookies, A. n.d. Data preparation - its applications and how it works. pp. 1-7.

Rediansyah, D., Prasojo, R. A. & Abu-Siada, A. 2021. Artificial intelligence-based power transformer health index for handling data uncertainty. *IEEE Access* 9: 150637-150648.

Sun, S. et al. 2020. Fault diagnosis of conventional circuit breaker contact system based on time-frequency analysis and improved AlexNet. *IEEE Transactions on Instrumentation and Measurement* 70: 1-12.

Taha, I. B. & Mansour, D. A. 2021. Novel power transformer fault diagnosis using optimized machine learning methods. *Intelligent Automation and Soft Computing* 28(3): 739-752.

Trimakno, D. & Kusrini. 2021. Impact of augmentation on batik classification using convolution neural network and K-nearest neighbor. In *ICOIACT 2021 - 4th International Conference on Information and Communications Technology: The Role of AI in Health and Social Revolution in Turbulence Era*, pp. 285-289.

Ullah, I., Khan, R. U., Yang, F. & Wuttisittikulkij, L. 2020. Deep learning image-based defect detection in high voltage electrical equipment. *Energies* 13(2): 392.

Zainoddin, M. H. S., Zainuddin, H. & Aman, A. 2017. Dielectrophoresis effect of dielectric liquids with suspended cellulose impurities under DC electric field. *International Journal of Electrical and Computer Engineering* 7(6): 3254-3261.